

## Local solutions to high-frequency 2D scattering problems

Andreas Asheim<sup>a,\*</sup>, Daan Huybrechs<sup>b,1</sup>

<sup>a</sup> NTNU Institute of Mathematical Sciences, 7491 Trondheim, Norway

<sup>b</sup> K.U. Leuven, Department of Computer Science, B-3001 Heverlee, Belgium

### ARTICLE INFO

#### Article history:

Received 3 June 2008

Received in revised form 4 February 2010

Accepted 24 March 2010

Available online 10 April 2010

#### Keywords:

Helmholtz problem

Integral equations

Oscillatory problems

Boundary layers

Filon-type method

### ABSTRACT

We consider the solution of high-frequency scattering problems in two dimensions, modeled by an integral equation on the boundary of a smooth scattering object. We devise a numerical method to obtain solutions on only parts of the boundary with little computational effort. The method incorporates asymptotic properties of the solution and can therefore attain particularly good results for high frequencies. We show that the integral equation in this approach reduces to an ordinary differential equation.

© 2010 Elsevier Inc. All rights reserved.

### 1. Introduction

Scattering problems in the domain exterior to a scattering surface are common in the modelling of electromagnetic and acoustic wave phenomena [21,44]. In these problems, the governing differential equation on the infinite domain surrounding the scattering obstacle can conveniently be replaced by an integral equation on the surface of the scatterer. The new computational domain is bounded and has lower dimension, two significant advantages for computational purposes. However, the numerical simulation of highly oscillatory phenomena remains a challenging problem. Traditional methods require a fine discretization in order to resolve the oscillations. Solution methods for partial differential equations may even require the degrees of freedom to grow faster than linearly with the frequency due to pollution errors [11]. A third advantage of boundary integral equations in an oscillatory setting is that they do not exhibit such errors [10]. Still, resolving the oscillations requires a fine discretization and this implies that the scattering problems rapidly become intractable as the frequency grows.

Although the situation improves with high-order methods for integral equations [16,27], the efficient implementation of fast multipole methods [46] or other approaches (see, for example, the overview in [13]), the computational complexity of these methods still increases with increasing frequency. Asymptotic methods on the other hand, such as Geometrical Optics, Physical Optics and the Geometric Theory of Diffraction [38], typically improve with increasing frequency [26]. They exhibit  $\mathcal{O}(k^{-n})$  error behaviour, where  $k$  is the wavenumber of the problem and  $n$  is a positive integer, though usually  $n = 1$ . Asymptotic methods have uncontrollable error for a fixed frequency however and, depending on the method, may exhibit breakdown near caustics or points of diffraction.

Recent research focuses on a combined, hybrid approach in the construction of converging boundary element methods that incorporate asymptotic properties of the solution (see [1,15,19,23], reviewed in [18]). This approach is most successful for scatterers with convex shape, but extends to multiple scattering configurations [24,3]. Some of the methods may be

\* Corresponding author. Tel.: +47 73 59 35 27; fax: +47 73 59 35 24.

E-mail address: [andreash@math.ntnu.no](mailto:andreash@math.ntnu.no) (A. Asheim).

<sup>1</sup> D. Huybrechs is a Postdoctoral Fellow of the Research Foundation Flanders (FWO).

implemented with a computational complexity that appears to be independent of the wavenumber for single convex obstacles [15,34] and multiple convex obstacles [28]. Although applicability is limited by the convexity requirements, the wavenumber independence motivates further research in this area. Other approaches for high-frequency scattering problems include using on-surface radiation conditions [25,37,4], which may lead to differential equations like in the current paper, and efficient preconditioners leading to convergent iterative methods at high frequencies [5,41] when coupled with fast multiple method techniques or hierarchical matrices [9].

Integral operators, being global operators, give rise to dense matrices upon discretization. This is however not compatible with the localization principle of high-frequency scattering problems, which states that the solution of the problem essentially depends on local properties of the scatterer [14]. The work in this paper was motivated by the observation that the method in [34], which applies to smooth scatterers, gives rise to a discretization matrix that is largely sparse if  $k$  is sufficiently large. Moreover, this method achieves high asymptotic order of accuracy in large parts of the computational domain. These two features are unique among the hybrid methods currently described in literature and represent a numerical manifestation of the localization principle. The result was obtained through a discretization based on Filon-type quadrature for highly oscillatory integrals [36] and does not require the construction of asymptotic expansions.

In this paper, we significantly extend the results and analysis of [34]. We restrict the computational domain to only a part of the boundary and we thereby relax convexity requirements. It turns out that, perhaps surprisingly, the integral equation in this setting reduces to an ordinary differential equation that is a singular perturbation problem. This equation can be solved rapidly and to essentially arbitrarily high asymptotic order of accuracy. The main achievement of the method is the computation of single reflections very efficiently and to high accuracy. This is by no means competitive with more general methods capable of treating arbitrary scattering configurations. Yet, owing to its simplicity and efficiency we believe it to be valuable in a range of applications. Moreover, we believe the reduction of a two-dimensional partial differential equation to a lower-dimensional integral equation and subsequently to a univariate ordinary differential equation to be interesting in its own right. A motivating application is the use of local solutions in iterative schemes for high-frequency scattering by multiple obstacles. Such schemes typically require in each step of the iteration the solution of a single scattering problem, in which only part of the computation is relevant for the next iteration [24,3]. Local solutions correspond exactly to such computations.

The layout of the paper is as follows. We start with a formal, non-theoretical description of the method in Section 2. The description differs from the method in [34] mostly in that the computational domain is truncated, which greatly simplifies computations. We analyze the asymptotic properties of our approach in Section 3. We give numerical results of a number of scattering problems in Section 4. Finally, we end with some concluding remarks in Section 5.

## 2. Description of the method

### 2.1. Problem statement

Consider a scattering object  $\Omega \in \mathbb{R}^2$  with a smooth boundary  $\Gamma = \partial\Omega$ . The total field surrounding the obstacle can be written as the sum of an incoming wave  $u^i$  and a scattered wave  $u^s$ . Our aim is to solve the two-dimensional Helmholtz equation for the scattered field in the exterior space,

$$\begin{aligned} \Delta u^s + k^2 u^s &= 0, & \mathbf{x} \in \mathbb{R}^2 \setminus \bar{\Omega}, \\ u^s(\mathbf{x}) &= -u^i(\mathbf{x}), & \mathbf{x} \in \Gamma. \end{aligned} \quad (2.1)$$

The Dirichlet boundary condition is such that the total field  $u^i + u^s$  vanishes on  $\Gamma$ , which corresponds to a perfectly reflecting object. The incoming wave  $u^i$  is assumed to be given. We further impose the Sommerfeld radiation condition on  $u^s$  in order to ensure uniqueness of the solution [21].

We can represent the unknown scattered wave with the *single-layer potential*

$$u^s(\mathbf{x}) = (Sq)(\mathbf{x}) = \int_{\Gamma} G(\mathbf{x}, \mathbf{y}) q(\mathbf{y}) d\mathbf{y}. \quad (2.2)$$

Here,  $q$  is the single-layer potential *density* and

$$G(\mathbf{x}, \mathbf{y}) = \frac{i}{4} H_0^{(1)}(k|\mathbf{x} - \mathbf{y}|) \quad (2.3)$$

is the Green's function of the two-dimensional Helmholtz equation. It is well known that the density function can be found from the integral equation of the first kind [21,44]

$$\int_{\Gamma} G(\mathbf{x}, \mathbf{y}) q(\mathbf{y}) d\mathbf{y} = -u^i(\mathbf{x}), \quad \mathbf{x} \in \Gamma. \quad (2.4)$$

Other integral formulations exist, and we note in particular the integral equation of the second kind

$$\frac{q(\mathbf{x})}{2} + \int_{\Gamma} \left( \frac{\partial G}{\partial n_x}(\mathbf{x}, \mathbf{y}) + i\eta G(\mathbf{x}, \mathbf{y}) \right) q(\mathbf{y}) d\mathbf{y} = \frac{\partial u^i}{\partial n}(\mathbf{x}) + i\eta u^i(\mathbf{x}), \quad (2.5)$$

with  $\eta \in \mathbb{R}$  a coupling parameter. Eq. (2.5) is uniquely solvable for all values of the wavenumber  $k$  [21]. It is important for further developments that the solution  $q$  in both cases corresponds to a physical density [15]. We proceed with Eq. (2.4) for simplicity of presentation, but the method was implemented for both equations. In the following, we assume a plane wave incidence or, more generally, an incoming wave of the form

$$u^i(\mathbf{x}) = -f(\mathbf{x})e^{ikg^i(\mathbf{x})}. \tag{2.6}$$

The function  $g^i(\mathbf{x})$  cannot be completely arbitrary however. Cases that we have in mind are waves arising from a point-source and waves that have already been reflected elsewhere.

### 2.2. Phase extraction and high-frequency formulation

As the wavenumber  $k$  increases the single-layer potential density  $q$  becomes increasingly oscillatory. In order to avoid a fine discretization grid, we will assume knowledge of the oscillatory behaviour of  $q$ . The main reason for the restriction to convex obstacles in literature is that the phase of the solution is then known to be the phase of the incoming wave. Let us write, for the time being indeed assuming a convex obstacle,

$$q(\mathbf{x}) = kq_s(\mathbf{x})e^{ikg^i(\mathbf{x})}. \tag{2.7}$$

It is known for a plane wave incidence that the function  $q_s$  is less oscillatory than  $q$  in the part of the computational domain that is “lit” by the incoming wave, and slowly oscillatory but rapidly decaying in the remainder [23]. This observation seems to hold for more general incoming waves as well. Thus, a coarser discretization can be used for  $q_s$  than for  $q$ . We introduced the normalizing factor  $k$  such that  $q_s = \mathcal{O}(1), k \rightarrow \infty$ .

The total phase of the integrand in (2.4) is given by the sum of the extracted phase of the solution and the phase of the Green’s function (2.3). It can be written as  $ikg_{tot}(\tau; t)$  where the oscillator  $g_{tot}$  is given by

$$g_{tot}(\tau; t) = g^i(\kappa(\tau)) - g^i(\kappa(t)) + d(t, \tau), \tag{2.8}$$

with

$$d(t, \tau) := |\kappa(t) - \kappa(\tau)|$$

the Euclidean distance between the two corresponding points on  $\Gamma$  [34].

Assume we have a smooth periodic parametrization of  $\Gamma$

$$\kappa(\tau) : [0, 1] \rightarrow \Gamma,$$

with  $|\nabla\kappa(\tau)| > 0$ . The integral Eq. (2.4) in terms of  $q_s$  becomes

$$(Kq_s)(t) = k \int_0^1 G_{no}(t, \tau)e^{ikg_{tot}(\tau; t)}q_s(\tau)d\tau = f(t), \quad t \in [0, 1], \tag{2.9}$$

with the singular but non-oscillatory function

$$G_{no}(t, \tau) := G(t, \tau)e^{-ikd(t, \tau)}|\nabla\kappa(\tau)|. \tag{2.10}$$

Note that in a slight abuse of notation we identified  $q_s(\kappa(\tau))$  with  $q_s(\tau), G(\kappa(t), \kappa(\tau))$  with  $G(t, \tau)$  and  $f(\kappa(t))$  with  $f(t)$ .

At first sight, the requirement of having a smooth parametrization seems to be rather restrictive, in particular with a generalization to three-dimensional problems in mind. On the other hand, the solution to high-frequency scattering problems is very sensitive to the shape of the boundary, and methods of high asymptotic order are meaningless when the shape of the boundary is insufficiently described.

### 2.3. Local solutions

The concept of local solutions of high-frequency scattering problems is based on the fact that local reflections are based (asymptotically) only on local data. In the following, we will consider an *admissible* part of the boundary and we are interested only in waves that are reflected once by this part of the boundary. First, we give the precise definition of an admissible part.

**Definition 2.1.** Consider a simply connected open subset  $\tilde{\Gamma} \subset \Gamma$  and a given incoming wave  $u^i$ . We say that  $\tilde{\Gamma}$  admits a local solution if

$$\frac{\partial g_{tot}}{\partial \tau}(\tau; t) \neq 0, \quad \forall t, \tau \in \kappa^{-1}(\tilde{\Gamma}). \tag{2.11}$$

Definition 2.1 is formulated in terms of the total oscillator function defined by (2.8). It excludes so-called *stationary points* of the integral  $Ku$  (see Section 2.4). In practice, this corresponds precisely to the exclusion of multiple reflections from  $\tilde{\Gamma}$  onto itself. The physical interpretation of Definition 2.1 therefore is that any part of  $\Gamma$  is admissible as long as the incoming wave reflecting from  $\tilde{\Gamma}$  does not immediately hit  $\tilde{\Gamma}$  again.

It is common in methods based on the technique of phase extraction to assume a convex boundary. Most of the theoretical results in asymptotic analysis moreover assume a plane wave incidence. Definition 2.1 is more general than these assumptions in two ways. First, the entire boundary need not be convex. For a plane wave incidence, any locally convex part of  $\Gamma$  is admissible, even when  $\Gamma$  itself is not convex. This is illustrated in the left panel of Fig. 1. Second, even local convexity is not required. If the given incoming wave does not reflect from  $\tilde{\Gamma}$  onto itself, then  $\tilde{\Gamma}$  is admissible. A non-convex admissible part is illustrated in the right panel of Fig. 1.

Next, we define the local solution. Let the interval  $[a, b]$  correspond to  $\kappa^{-1}(\tilde{\Gamma})$ , where  $\tilde{\Gamma}$  admits a local solution according to Definition 2.1. This will be our computational domain. If the obstacle  $\Omega$  is such that no multiple reflection occurs, then we simply define the local solution to be

$$q_l(t) = q_s(t), \quad t \in [a, b], \tag{2.12}$$

i.e., the local solution is the restriction of the density function  $q_s$  to  $[a, b]$ . If the obstacle  $\Omega$  gives rise to multiple reflections, consider a different obstacle  $\tilde{\Omega}$  such that  $\tilde{\Gamma}$  is an admissible part of its boundary and no multiple reflections occur. Then the local solution is defined to be

$$q_l(t) = \tilde{q}_s(t), \quad t \in [a, b], \tag{2.13}$$

where  $\tilde{q}_s$  is the solution of the scattering problem on the boundary of  $\tilde{\Omega}$ . Suitable choices of obstacles  $\tilde{\Omega}$  are shown in Fig. 1 for both examples. In practice, a suitable obstacle  $\tilde{\Omega}$  is never constructed in the numerical method.

#### 2.4. Application of Filon-type quadrature

The integral Eq. (2.9) after phase extraction has a highly oscillatory integral in the left hand side. Our computational method is based on an efficient numerical method to evaluate oscillatory integrals, namely Filon-type quadrature [36]. We refer the reader to [31] for a review of this and other modern numerical methods for evaluating highly oscillatory integrals.

##### 2.4.1. Filon-type quadrature

Many highly oscillatory integrals of practical interest have the general form

$$I[f] := \int_a^b f(\tau) e^{ikg(\tau)} d\tau, \tag{2.14}$$

where both  $f$  and  $g$  are non-oscillatory functions and the parameter  $k$  is large. Filon-type quadrature is an effective quadrature approximation  $Q[f]$  to  $I[f]$  using derivatives with the general form

$$I[f] \approx Q[f] := \sum_{l=1}^N \sum_{j=0}^{J_l} w_{l,j} f^{(j)}(\tau_l). \tag{2.15}$$

The quadrature points  $\tau_l, l = 1, \dots, N$ , include the endpoints  $a$  and  $b$  and any singular points of  $f$  and  $g$ , as well as the stationary points, these are all points  $\xi \in (a, b)$  such that  $g'(\xi) = 0$ . The method is based on polynomial interpolation of the non-oscillatory function  $f$ , which ensures possible convergence for any value of  $k$  simply by adding quadrature points. The use of derivatives of  $f$  at endpoints and stationary points also ensures high asymptotic order of accuracy, in the sense that

$$I[f] - Q[f] = \mathcal{O}(k^{-d}), \quad k \rightarrow \infty,$$

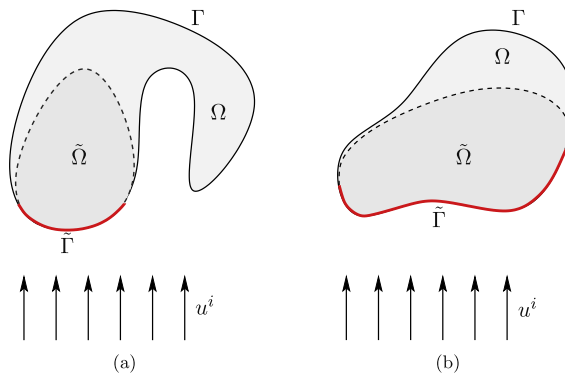


Fig. 1. Examples of non-convex domains. The highlighted part  $\tilde{\Gamma}$  of the boundary  $\Gamma$  admits a local solution. The dashed curve indicates an extension of  $\tilde{\Gamma}$  to the boundary of an obstacle  $\tilde{\Omega}$ . The local solution is asymptotic to the solution of the scattering problem involving  $\tilde{\Omega}$ , restricted to  $\tilde{\Gamma}$ .

where  $d > 0$  depends on the number of derivatives  $J_l, l = 1, \dots, N$ , used and on the order of the stationary points [36]. A stationary point has higher order if in addition to  $g'(\xi) = 0$  higher order derivatives of  $g$  also vanish.

2.4.2. Application to the full scattering problem

Filon-type quadrature was used to solve the full scattering problem for convex obstacles in [34], based on the observation that the operator  $K$  yields an oscillatory integral of the form (2.14) for each value of  $t$ . In particular, the oscillator is given by  $g_{tot}(\tau; t)$  as a function of  $\tau$  for fixed  $t$ . The integral  $Ku$  can therefore be approximated by Filon-type quadrature where both the weights and the quadrature points now depend on the value of  $t$ :

$$(Ku)(t) \approx \sum_{l=1}^N \sum_{j=0}^n w_{l,j}(t) u^{(j)}(\tau_l(t)). \tag{2.16}$$

It was shown in [34] that this quadrature approximation too has high asymptotic accuracy. It may be used to solve Eq. (2.9), i.e.,  $Kq_s = f$ . However, an inherent assumption of Filon-type quadrature for  $Ku$  is that  $u$  is non-oscillatory. As noted earlier, the solution  $q_s$  may be oscillatory in certain parts of the domain and, hence, different discretization of  $Ku$  has to be applied in those regions. Approximation (2.16) can only be applied when  $\kappa(t)$  is in the region lit by the incoming wave.

2.4.3. Application to the local problem

The approach simplifies considerably in the setting of local solutions. In particular, fewer quadrature points are necessary. Note that the integrand of  $Ku$  is smooth except for the singularity of the Green’s function when  $t = \tau$ . This point produces a contribution to the asymptotic expansion of the integral [47,45] and should therefore be included as a quadrature point. Stationary points on  $\tilde{\Gamma}$  are excluded by construction according to Definition 2.1. Stationary points elsewhere physically correspond to multiple reflections and they are simply discarded. Thus, the only contributing point is  $\tau = t$  and the Filon-type quadrature simplifies to

$$(Ku)(t) \approx (Q_n u)(t) := \sum_{j=0}^n w_j(t) u^{(j)}(t), \quad t \in [a, b]. \tag{2.17}$$

We replace the integral operator  $K$  by its Filon-type quadrature approximation in Eq. (2.9). The local method consists of solving the equation

$$(Q_n q_F)(t) = f(t), \quad t \in [a, b]. \tag{2.18}$$

We call a solution  $q_F$  to this problem a Filon solution.

2.4.4. The weights of Filon-type quadrature

The weights of an interpolatory quadrature rule correspond to the integrals of Lagrangian interpolants [22]. The weights of quadrature rules using derivatives are similar, but based on Hermite interpolation. To be precise, weight  $w_{l,j}$  in (2.15) for the evaluation of the model integral (2.14) is given by

$$w_{l,j} := I[p_{lj}],$$

with  $p_{lj}$  the Hermite interpolating polynomial that satisfies

$$p_{lj}^{(k)}(\tau_m) = \delta_{l-m} \delta_{j-k}.$$

Note that the weights correspond to oscillatory integrals themselves. This is a general issue when using Filon-type quadrature. In our implementation, we have evaluated the weights using the steepest descent technique proposed in [32], which is a numerical adaptation of the classical method of steepest descent [47]. The weights are then given by a sum of line integrals along the paths of steepest descent of the total oscillator  $g_{tot}$ .

The evaluation of the specific oscillatory integral appearing in (2.9) requires only minor changes to the general method, which we now discuss. Since the oscillator  $g_{tot}(\tau; t)$  has a square root singularity at  $\tau = t$ , there are two paths of steepest descent in the complex plane that originate in  $t$ , corresponding to the two solutions  $h(p)$  of the general path equation

$$g_{tot}(h(p); t) = g_{tot}(t; t) + ip = ip. \tag{2.19}$$

Each solution  $h(p)$  results in a non-oscillatory integral with exponential decay, since the above equation implies that

$$e^{ikg_{tot}(h(p);t)} = e^{ik(g_{tot}(t;t)+ip)} = e^{-kp}.$$

Call these solutions  $h_1(p)$  and  $h_2(p)$ . Since in the setting of local solutions only the contributing point  $\tau = t$  is kept, it is sufficient to consider only the polynomials  $\frac{1}{j!}(\tau - t)^j$ , instead of the full set of Hermite interpolating polynomials [32]. We arrive at a definition of the weights in (2.17) as follows:

$$w_j(t) = -\frac{1}{j!} k \int_0^\infty G_{no}(t, h_1(p))(h_1(p) - t)^j h_1'(p) e^{-kp} dp + \frac{1}{j!} k \int_0^\infty G_{no}(t, h_2(p))(h_2(p) - t)^j h_2'(p) e^{-kp} dp. \tag{2.20}$$

In the first integral we used the analytic continuation of the integrand for  $\tau < t$ , in the second integral we use the analytic continuation corresponding to  $\tau > t$ . This also fixes the choice of  $h_1$  and  $h_2$ .

The two line integrals above have a logarithmic singularity at  $p = 0$ . A new element in our implementation, compared to the technique described in [34], is that the integrals are evaluated with generalized Gaussian quadrature. Suitable quadrature rules for exponentially decaying integrands with a logarithmic singularity were constructed with this particular application in mind in §7, Example 2, of [30].

Note that we have assumed analyticity of the integrand, and in particular of the parametrization  $\kappa(t)$  of the boundary  $\Gamma$ . The upper integration limit  $\infty$  in (2.20) may be replaced by any finite value  $P > 0$  that is independent of  $k$ . Alternatively, one could define suitable weights by

$$w_j(t) = k \int_0^1 G_{no}(t, \tau) e^{ikg_{tot}(\tau; t)} \frac{1}{j!} (\tau - t)^j \chi(\tau) d\tau, \quad (2.21)$$

where  $\chi(\tau)$  is a smooth cut-off function that equals 1 in a small neighbourhood of  $t$ . The equivalence of this definition will be shown further on in Lemma 3.4. This approach avoids complex arithmetic and analyticity assumptions. This resembles the approach taken in [15], but a useful difference is that the current approach achieves high asymptotic order in  $k$ .

Finally, we note that the weights rapidly decrease in size for derivatives of increasing order. In particular, it follows from [34, Lemma 3.3] that <sup>1</sup>

$$w_j(t) = \mathcal{O}(k^{-j}), \quad k \rightarrow \infty. \quad (2.22)$$

#### 2.4.5. Discretization

For the numerical solution we introduce a discrete space and solve Eq. (2.18) based on collocation. Let  $V_h$  be a discrete space spanned by a set of  $N$  basis functions  $\{\phi_j\}_{j=1}^N$ . A function in  $V_h$  can be represented by a set of  $N$  coefficients  $\mathbf{c} = \{c_j\}_{j=1}^N$  through the operator

$$L_h : \mathbb{C}^N \rightarrow V_h, \quad L_h \mathbf{c} = \sum_{j=1}^N c_j \phi_j.$$

Furthermore, a set of  $N$  collocation points  $\{t_j\}_{j=1}^N$  is needed and we define the corresponding evaluation operator

$$\Pi_h : W \rightarrow \mathbb{C}^N, \quad \Pi_h f = \{f(t_j)\}_{j=1}^N.$$

With this notation, the discretization matrix is found to be

$$M = \Pi_h Q_n L_h. \quad (2.23)$$

An approximation to the solution of (2.18) is found by solving

$$M \mathbf{c} = \Pi_h f =: \mathbf{b}. \quad (2.24)$$

We denote by

$$q_h(t) = L_h \mathbf{c} \in V_h \quad (2.25)$$

the numerical solution.

In our implementation we chose  $V_h$  to be the space of natural splines of (odd) order  $s$ . The nodes of the splines were taken as collocation points. We note that the dimension of the space of splines is in general higher than the number of nodes. Natural splines remove a number of degrees of freedom by requiring vanishing high-order derivatives at the endpoints. We will elaborate on the importance of this boundary condition in Section 3.

The system (2.24) is typically very small because the computations involve only a part of the scatterer. We have therefore used a direct solver. Following [40,20], we have chosen the coupling parameter  $\eta$  in (2.5) to be  $\eta = k$  in order to minimize the condition number, though we found condition numbers to be small for all examples in this paper, including for the integral equation of the first kind (2.4). Interestingly, the choice  $\eta = k$  can be seen as corresponding to a low-order approximation of the Dirichlet-to-Neumann operator at high frequencies [5,6]. Based on our numerical experiments however, we found that this formulation based on an integral equation of the second kind seems to yield less accurate solutions.

### 3. Analysis

Numerical results of the method to compute local solutions will be given in Section 4. The results indicate that the accuracy of the computed solution  $q_h$  increases rapidly with increasing frequency throughout the computational domain,

$$q_h(t) - q_s(t) = \mathcal{O}(k^{-n-1}), \quad \forall t \in [a, b]. \quad (3.1)$$

<sup>1</sup> The asymptotic order of the weights as displayed here is a factor  $k$  larger than what is given in [34] due to the normalizing factor  $k$  in (2.7).

This behaviour is reminiscent of asymptotic expansions, but unlike traditional boundary element methods for oscillatory integral equations. In this section we shall give a partial proof of this result based on rigorous results in asymptotic analysis, completed with arguments based on the (non-rigorous) theory of singularly perturbed differential equations.

Rigorous mathematical results on the asymptotic behaviour of scattering solutions are known, with few exceptions, only for convex obstacles and incident plane waves (see [23] and references therein). For this reason, throughout this section we shall assume that  $\Omega$  is a convex obstacle, and restrict ourselves to the case of an incident plane wave,

$$u^i(\mathbf{x}) = e^{i\mathbf{k}\mathbf{x}\cdot\mathbf{d}},$$

where the direction vector  $\mathbf{d}$  has unit length. We do note, however, that our numerical results indicate a similar behaviour for the more general obstacles shown in Fig. 1 with  $\Omega$  replaced by  $\tilde{\Omega}$  and for more general incoming waves.

### 3.1. Asymptotic properties of the solution

We start with a description of the asymptotic behaviour of the slowly oscillatory function  $q_s(t)$  that solves Eq. (2.9). This behaviour is well understood and differs in different parts of the obstacle. For a convex obstacle and plane wave incidence, there are two points where the incoming wave is tangent to the boundary. We denote those by  $s_1$  and  $s_2$  respectively, and we let  $t_1$  and  $t_2$  be the corresponding points in the parameter domain, i.e.,  $\kappa(t_{1,2}) = s_{1,2}$ . We assume without loss of generality that  $t_1 < t_2$  and we define the illuminated region

$$\Gamma_i = (t_1, t_2)$$

and the shadow region

$$\Gamma_s = [0, 1] \setminus \overline{\Gamma_i}.$$

In the illuminated region, the first order asymptotic term is commonly known as the Kirchhoff approximation or Physical Optics approximation. For the incident plane wave and assuming a natural parametrization  $\kappa(t)$  of  $\Gamma$ , it is given explicitly by

$$q_s(t) \sim 2i\mathbf{v}(\kappa(t)) \cdot \mathbf{d}, \quad k \rightarrow \infty, \quad t \in \Gamma_i, \tag{3.2}$$

where  $\mathbf{v}(\mathbf{x})$  is the exterior normal to  $\Gamma$  at  $\mathbf{x} \in \Gamma$ . More generally, the solution  $q_s(t)$  has a full asymptotic expansion of the form

$$q_s(t) \sim \sum_{j=0}^{\infty} a_j(t) k^{-j}, \quad k \rightarrow \infty, \tag{3.3}$$

for all points  $t$  in  $\Gamma_i$ . The functions  $a_j(t)$  are  $C^\infty$  and independent of  $k$ . They can be constructed explicitly for all sufficiently smooth and convex scatterers. Examples of such computations are given in [17] and in [8, Ch. 1]. It follows from these constructions that the  $a_j(t)$  depend only locally on the surface, i.e., on the tangent, curvature, and higher derivatives at  $\kappa(t)$ . This is commonly called the *localization principle* of high-frequency scattering. A mathematical justification for these formal constructions is given in [43] for the case of Dirichlet boundary conditions.

It follows from (3.3) that  $q_s$  and all its derivatives are bounded in  $k$  in the illuminated region. In the shadow region the function  $q_s$  is known to exhibit *extra-polynomial decay*, i.e., faster than any inverse power of  $k$  (see e.g. [43, Sect. 2]). Note that a slightly stronger result can be proved, namely that

$$\|q\|_{L_2(A_2)} \leq c' \exp(-ck^\delta).$$

This result is stated in [23, Theorem 6.5] with several references to rigorous proofs. We shall here only employ the property of extra-polynomial decay, which is a slightly weaker result.

Finally, the function  $q_s$  has large derivatives in a region around the shadow boundary that shrinks like  $k^{-1/3}$ . A useful global bound on the derivatives of  $q_s$  was established in [23, Corollary 5.5],

**Lemma 3.1.** For all  $n \geq 1$ ,

$$\left| \frac{d^n q_s}{d\tau^n}(\tau) \right| = \mathcal{O}((k^{(n-1)/3}), \quad t \in [0, 1].$$

This bound is sharp in the shadow boundary region, but pessimistic in both the illuminated and shadow regions.

### 3.2. Asymptotic order of accuracy of $q_F$

We set out to show that the Filon solution  $q_F$  is asymptotically close to the exact solution  $q_s$ . First, we gather some useful lemmas. Next, in Theorem 3.5 we prove that  $Q_n$  is a good asymptotic approximation to  $K$ , in the sense that both operators applied to the exact solution  $q_s$  agree to high asymptotic order. The argument will finally be completed in Section 3.3.

3.2.1. Stationary points

As indicated in Section 2.4.1, the asymptotic behaviour of an oscillatory integral depends critically on its stationary points. In the following we will need to know some specifics about the location of the stationary points of the integral (2.9).

**Lemma 3.2.** For  $t \in \Gamma_i$ , the stationary points of the integral (2.9), i.e., the zeros of the derivative of (2.8), are all contained in  $\Gamma_s$ .

**Proof.** Performing the differentiation yields,

$$\frac{\partial g_{tot}}{\partial \tau}(\tau; t) = (\mathbf{v}(\tau, t)^T + \mathbf{d}^T) \cdot \nabla \kappa(\tau),$$

where,

$$\mathbf{v}(\tau, t) = \frac{\kappa(\tau) - \kappa(t)}{\|\kappa(\tau) - \kappa(t)\|}.$$

We have  $|\mathbf{v}| \equiv |\mathbf{d}| = 1$  and  $\mathbf{v}(\tau, t)$  is discontinuous at  $\tau = t$  with left and right limits  $\pm \nabla \kappa(\tau)^T / \|\nabla \kappa(\tau)\|$ . Thus, a stationary point can only occur if either  $\mathbf{v} = -\mathbf{d}$  or if  $\mathbf{v} + \mathbf{d} \perp \nabla \kappa$ .

We first rule out the former case. The vector  $\mathbf{v}$  points from  $\kappa(t)$  to  $\kappa(\tau)$ , which implies that  $\mathbf{v} = -\mathbf{d}$  can only occur along the line parallel to  $\mathbf{d}$  passing through  $\kappa(t)$ . Because of convexity there can be no point of  $\Gamma$  in the direction  $-\mathbf{d}$  when  $\tau \in \Gamma_i$ .

Next, we consider the points  $\tau$  for which  $(\mathbf{v}(\tau, t) + \mathbf{d}) \perp \nabla \kappa$ . Let  $\phi_1$  be the angle between  $\mathbf{d}$  and the normal  $\nu$  at  $\kappa(\tau)$ , and  $\phi_2$  the angle between  $\mathbf{v}$  and  $\nu$ . Since both  $\mathbf{v}$  and  $\mathbf{d}$  have unit length, for the orthogonality condition to hold we should have either  $\phi_1 = -\phi_2$  or  $\phi_1 = \phi_2 + \pi$  (in both cases modulo  $2\pi$ ). The latter case implies  $\mathbf{v} = -\mathbf{d}$ , which was already ruled out above. In the former case, it follows that  $\mathbf{d}$  and  $-\mathbf{v}$  make equal angles with the normal at  $\kappa(\tau)$ . Thus, an incident ray in the direction of  $\mathbf{d}$  at  $\kappa(\tau)$  would reflect in the direction of  $-\mathbf{v}$ . But  $-\mathbf{v}$  points towards  $\kappa(t)$  and this scenario clearly can not occur for  $\tau \in \Gamma_i$ ; all incident rays will reflect away from  $\Omega$ .  $\square$

Note that in the proof of Lemma 3.2 we encountered a special case of a more general principle, namely that stationary points of the integral (2.9) correspond to double reflections. This is illustrated in the right panel of Fig. 2: if a wave in the direction of  $d$  hits the obstacle at a point  $\kappa(\tau)$  and reflects to hit the obstacle again at the point  $\kappa(t)$ , then  $\tau$  is a stationary point for  $t$ .

3.2.2. Localizing the integral operator

Next, we localize the integral  $Kq_s$  around the singularity of the integrand by introducing a cut-off function and we show that the remainder of the integral is asymptotically small.

We split the integral in different regions using a partition of unity as follows. Let  $A_1$  be a sub interval of  $\Gamma_i$  such that  $t \in A_1$ . Next, as a consequence of Lemma 3.2 we can find a subset  $A_2 \subset \Gamma_s$  of the shadow region that contains all stationary points in its interior. Finally, we construct two intervals  $A_3$  and  $A_4$  around the shadow boundaries  $t_1$  and  $t_2$  respectively, that intersect  $A_1$  and  $A_2$ , but such that there are no stationary points in  $A_{3,4}$  and such that  $t \in A_1 \setminus (A_3 \cup A_4)$ . The partition of unity is constructed as a collection of functions  $\chi_j \in C^\infty, j = 1, \dots, 4$  such that,

$$\text{supp}(\chi_j) = A_j, \quad 0 \leq \chi_j(\tau) \leq 1, \quad \text{and} \quad \sum_{j=1}^4 \chi_j(\tau) = 1.$$

Denote by  $\tilde{K}$  the localized integral operator defined as

$$\tilde{K}(u) = K(\chi_1 u). \tag{3.4}$$

We have the following result.

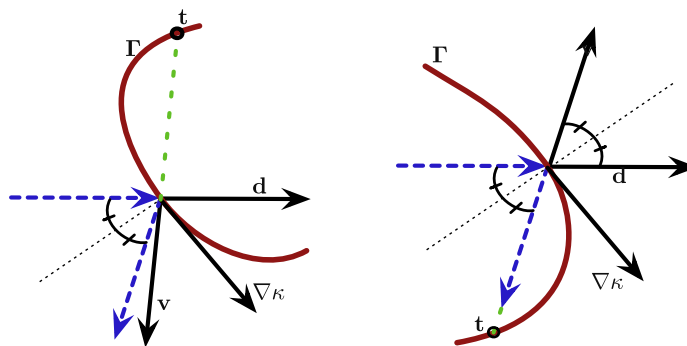


**Fig. 2.** An illustration for the proof of Lemma 3.2. Left: A ray reflects away from a convex obstacle, whereas  $-\mathbf{v}$  points into the obstacle. Right: A non-convex configuration allows stationary points.

**Lemma 3.3.** For  $t \in \Gamma_i$ ,

$$K(q_s) - \tilde{K}(q_s) = \mathcal{O}(k^{-N}), \quad \forall N \in \mathbb{N}.$$

**Proof.** The difference between the two integral operators is

$$K(q_s) - \tilde{K}(q_s) = k \sum_{j=2}^4 \int_{\mathcal{A}_j} G_{no}(t, \tau) e^{ikg_{tot}(\tau;t)} \chi_j(\tau) q_s(\tau) d\tau.$$

The integral over  $\mathcal{A}_3$  contains no stationary points by construction. Thus, we can perform repeated integration by parts, as is usually done for oscillatory integrals of the form (2.14) without stationary points. The boundary terms will drop out since  $\chi_3$  and all its derivatives vanish at the boundaries. Performing integration by parts  $m$  times yields (see e.g. [7, Sect. 2])

$$\int_{\mathcal{A}_3} G_{no}(t, \tau) e^{ikg_{tot}(\tau;t)} \chi_3(\tau) q_s(\tau) d\tau = \frac{1}{(-ik)^m} \int_{\mathcal{A}_3} \sigma_m[F_3 q_s](\tau) e^{ikg_{tot}(\tau;t)} d\tau, \tag{3.5}$$

where the functions  $\sigma_j$  are defined recursively,

$$\begin{aligned} \sigma_0[f](\tau) &= f(\tau), \\ \sigma_{j+1}[f](\tau) &= \frac{d}{d\tau} \frac{\sigma_j[f](\tau)}{g'(\tau)}, \quad k = 0, 1, \dots, \end{aligned}$$

and  $F_3$  is the non-oscillatory function

$$F_3(\tau; t) = G_{no}(t, \tau) \chi_3(\tau).$$

Boundedness of this function and its partial derivatives for increasing  $k$  when  $t \neq \tau$  follows readily from the asymptotic expansion of the Hankel function for large arguments [2].

In [36] it is shown that the functions  $\sigma_m$  depend on the derivatives of  $f$  in a predictable manner, namely that there exist functions  $\sigma_{m,j}(x), \sigma_{m,m}(x) \neq 0$ , depending on  $g_{tot}$  and its derivatives, such that,

$$\sigma_m[f](x) = \sum_{j=0}^m \sigma_{m,j}(x) f^{(j)}(x). \tag{3.6}$$

Note that from the construction of  $\mathcal{A}_3$  the function  $F_3$  is  $C^\infty(\mathcal{A}_3)$ . As a consequence of Leibniz' Rule, Eq. (3.6) and Lemma 3.1 we then get, for  $m \geq 1$ ,

$$\sigma_s[F_3](x) = \sum_{j=0}^m \sigma_{s,j}(x) \frac{\partial^j}{\partial \tau^j} [F_3(\tau; t) q_s(\tau)] = \mathcal{O}(k^{(m-1)/3}).$$

Using this result to bound the integral on the right hand side of (3.5) we get that the left hand integral is  $\mathcal{O}(k^{-(2m-1)/3})$  for all  $m \geq 1$ , or equivalently,

$$\int_{\mathcal{A}_3} G_{no}(t, \tau) e^{ikg_{tot}(\tau;t)} \chi_3(\tau) q_s(\tau) d\tau = \mathcal{O}(k^{-N}), \quad \forall N \in \mathbb{N}.$$

The reasoning for  $\mathcal{A}_4$  is similar. This leaves the integral over  $\mathcal{A}_2$ . Here we use the fact that  $K(t, \tau)$  is bounded as a function of  $\tau$  in  $\mathcal{A}_2$ , which gives

$$\int_{\mathcal{A}_2} G_{no}(t, \tau) e^{ikg_{tot}(\tau;t)} \chi_2(\tau) q_s(\tau) d\tau \leq C \sup_{\tau \in \mathcal{A}_2} [q_s(\tau)] = \mathcal{O}(k^{-N}),$$

where the last equality is a consequence of the extra-polynomial decay of the solution in the shadow zone. This concludes the proof.  $\square$

Finally, we show that the definition of the weights using steepest descent paths as in (2.20) or using a cut-off function as in (2.21) are indeed asymptotically equivalent.

**Lemma 3.4.** Let  $\chi_1$  and  $\tilde{K}$  be defined as above and  $w_j(t)$  defined by (2.20). Then

$$w_j(t) = K \left( \chi_1 \frac{1}{j!} (\tau - t)^j \right) + \mathcal{O}(k^{-N}), \quad \forall N \in \mathbb{N}.$$

**Proof.** The technical challenge here is that  $\chi_1$  is not analytic, which prevents immediate application of Cauchy's theorem. On the other hand, the singularity of the kernel prevents immediate application of integration by parts. We proceed by carefully removing the singularity from the problem.

Assume that  $[c_1, c_2] = \Gamma_1$  is the support of  $\chi_1$  and  $\chi_1(\tau) \equiv 1$  on  $[d_1, d_2] \subset [c_1, c_2]$ . By construction we have  $t \in [d_1, d_2]$ . We focus on the interval  $[t, c_2]$  and note that the reasoning for  $[c_1, t]$  is similar. We fix  $t$  and define

$$U(\tau) = kG_{no}(t, \tau)e^{ikg_{tot}(\tau; t)}.$$

Under the same conditions as the validity of (2.20), the integral

$$I_1 := \int_t^{d_2} U(\tau) \frac{1}{j!} (\tau - t)^j \chi_1(\tau) d\tau = \int_t^{d_2} U(\tau) \frac{1}{j!} (\tau - t)^j d\tau = \int_{L_1} U(z) \frac{1}{j!} (z - t)^j dz - \int_{L_2} U(z) \frac{1}{j!} (z - t)^j dz$$

can be written as the sum of two line integrals in the complex plane, with  $L_1$  and  $L_2$  the steepest descent paths at  $t$  and  $d_2$  respectively. Note that the integral along  $L_1$  is precisely the second integral of  $w_j(t)$  in (2.20).

Next, we define the integral

$$I_2 := \int_{d_2}^{c_2} U(\tau) \chi_1(\tau) \frac{1}{j!} (\tau - t)^j d\tau.$$

We aim to show that the integral along  $L_2$  above cancels with  $I_2$ . A similar reasoning on  $[c_1, t]$  would then complete the proof.

To that end, consider an analytic function  $\psi(\tau)$  such that

$$\psi(\tau) = 1 + \mathcal{O}((\tau - d_2)^M), \quad \tau \rightarrow d_2, \quad \text{and}$$

$$\psi(\tau) = \mathcal{O}((\tau - c_2)^M), \quad \tau \rightarrow c_2,$$

for an integer  $M$ . The integral

$$I_3 := \int_{d_2}^{c_2} U(\tau) \psi(\tau) \frac{1}{j!} (\tau - t)^j d\tau = \int_{L_2} U(z) \psi(z) \frac{1}{j!} (z - t)^j dz - \int_{L_3} U(z) \psi(z) \frac{1}{j!} (z - t)^j dz$$

can also be written as the sum of two steepest descent line integrals, where  $L_2$  is the same path as before and  $L_3$  originates in  $\tau = c_2$ . From [34, Lemma 3.3] we deduce that, for sufficiently large  $M$ , the integral along  $L_2$  agrees with the former integral along  $L_2$  to high asymptotic order (because the Taylor series of both integrands around  $d_2$  agree to high order) and that the integral along  $L_3$  vanishes to high asymptotic order. Finally, integration by parts as in the proof of the previous lemma shows that  $I_2$  and  $I_3$  also agree to high asymptotic order. This concludes the proof.  $\square$

### 3.2.3. Asymptotic accuracy of $Q_n$

We have established enough results to prove the following theorem, which shows that it makes sense to approximate the integral operator  $K$  by the differential operator  $Q_n$ .

**Theorem 3.5.** For  $t \in \Gamma_i$ ,

$$(Kq_s)(t) - (Q_n q_s)(t) = \mathcal{O}(k^{-n-1}), \quad \forall t \in [a, b].$$

**Proof.** We may conclude from Lemmas 3.3 and 3.4 and from the definition (2.17) of  $Q_n$  that it is sufficient to prove

$$k \int_{\mathcal{A}_1} G_{no}(t, \tau) e^{ikg_{tot}(\tau; t)} \chi_1(\tau) \left( q_s(\tau) - \sum_{j=0}^n q_s^{(j)}(t) \frac{(\tau - t)^j}{j!} \right) = \mathcal{O}(k^{-n-1}).$$

This expression implies that the  $k$ th term of the asymptotic expansion of the oscillatory integral  $\tilde{K}q_s$  depends on the  $k$ th order derivative of  $q_s$  at the single contributing point  $t$ : subtracting out derivatives renders the integral asymptotically smaller.

This is most easily proved using integration by parts, as was done for integrals over  $\Gamma_3$  in the proof of Lemma 3.3. The integral over  $\Gamma_1$  is slightly more involved due to the singularity at  $\tau = t$ . However, we can write

$$q_s(\tau) - \sum_{j=0}^n q_s^{(j)}(t) \frac{(\tau - t)^j}{j!} = \sum_{j=n+1}^M q_s^{(j)}(t) \frac{(\tau - t)^j}{j!} + R_M(\tau), \quad (3.7)$$

where the remainder term  $R_M(\tau)$  vanishes to high order at  $\tau = t$ . Recall that  $q_s$  and its derivatives, hence also  $R_M$  and its derivatives, are bounded in  $k$ . Substituting into the above, we conclude from Lemma 3.4 that each term in the Taylor series of  $q_s$  gives rise to an integral that is  $\mathcal{O}(k^{-n-1})$  or smaller. The integral involving  $R_M(\tau)$  can also be bounded by  $\mathcal{O}(k^{-n-1})$  by performing integration by parts  $n + 2$  times and noting that all boundary terms in the process vanish. The integrand is sufficiently differentiable at  $\tau = t$  if  $M$  is taken sufficiently large.  $\square$

### 3.3. A singular perturbation problem

Let us analyze the form of Eq. (2.18), which we repeat here for the clarity of our exposition:

$$\sum_{j=0}^n w_j(t) q_F^{(j)}(t) = f(t), \quad t \in [a, b]. \tag{3.8}$$

This is an ordinary differential equation of order  $n$ , rather than an integral equation. Note that no boundary conditions are specified. Since the local solution is a restriction of the full solution of the scattering problem to a part of the domain, it seems impossible to determine  $n$  boundary conditions without prior knowledge of the full solution.

However, the differential Eq. (3.8) has a special form. Recall that the variable coefficients in this ODE have size  $w_j(t) = \mathcal{O}(k^{-j})$  as  $k \rightarrow \infty$ . Thus, (3.8) has the form of a *singular perturbation problem* (see, for example, [12]):

$$\varepsilon^n v_n(t) q_F^{(n)}(t) + \dots + \varepsilon v_1(t) q_F'(t) + v_0(t) q_F(t) = f(t), \quad t \in [a, b],$$

with  $\varepsilon \sim 1/k$  a small parameter and  $v_j(t) = \mathcal{O}(1)$  as  $\varepsilon \rightarrow 0$ . The solution to such a problem can be written as the sum of a slowly and rapidly varying part,

$$q_F(t) = q_S(t) + q_R(t), \quad t \in [a, b].$$

The rapidly varying part  $q_R(t)$  depends on the boundary conditions for  $q_F$ , but manifests itself only in *boundary layers* near the endpoints of the interval. It vanishes rapidly in the interior. The slowly varying part is smooth everywhere and independent of the boundary conditions. A first order approximation is  $q_S(t) \sim f(t)/v_0(t)$ .

The solution to (3.8) of interest is non-oscillatory on  $[a, b]$  and therefore corresponds to the slowly varying solution  $q_S(t)$  above. This function  $q_S(t)$  has bounded derivatives in  $\varepsilon$  at the endpoints. Then the *bounded derivative principle* [39] applies: if boundary conditions are chosen such that derivatives up to order  $p$  are bounded in  $\varepsilon$  at the boundary, then the boundary data is correct for  $q_S$  to order  $p$ . The function  $q_S$  can moreover be determined to any asymptotic order in the interior  $(a, b)$ . Thus, even if boundary values of the solution are not specified, enforcing bounded derivatives at the endpoints ensures that the slowly varying part of the solution can be recovered to a certain asymptotic order in  $\varepsilon$ .

Using the theory of singularly perturbed differential equations, we may fully explain the observed asymptotic accuracy of  $q_F$ . In order to recover a non-oscillatory solution to (3.8), we augment this equation with the condition that derivatives of  $q_F$  are bounded in  $k$ :

$$q_F^{(j)}(t) = \mathcal{O}(1), \quad k \rightarrow \infty, \quad j = 0, \dots, n. \tag{3.9}$$

We have, for any  $N \in \mathbb{N}$  and  $t \in [a, b]$ ,

$$\sum_{j=0}^n w_j(t) [q_S^{(j)}(t) - q_F^{(j)}(t)] = (Q_n q_S)(t) - (Q_n q_F)(t) = (K q_S)(t) + \mathcal{O}(k^{-n-1}) - f(t) = \mathcal{O}(k^{-n-1}).$$

Both  $q_F$  and  $q_S$  have  $\mathcal{O}(1)$  derivatives as  $k \rightarrow \infty$ . Comparing the asymptotic size of all terms in the summation to the right hand side, and using  $w_j = \mathcal{O}(k^{-j})$ , gives

$$q_F^{(j)}(t) = q_S^{(j)}(t) + \mathcal{O}(k^{j-n-1}), \quad j = 0, \dots, n.$$

We therefore expect that the functions  $q_F$  and  $q_S$  agree to asymptotic order  $n + 1$ , and higher order derivatives agree to lower asymptotic order.

Natural splines are a convenient choice to enforce (3.9) because they satisfy homogeneous boundary conditions in high-order derivatives at the endpoints. In particular, using natural splines of odd degree  $s$  we have

$$\forall v \in V_h : v^{(j)}(a) = v^{(j)}(b) = 0, \quad j = \frac{s+1}{2}, \dots, s-1.$$

Enforcing boundary conditions on higher derivatives independently of  $k$  ensures that lower derivatives are bounded in  $k$  and, hence, by the bounded derivative principle we find the correct solution to high asymptotic order. The solution in the interior has full asymptotic accuracy  $n + 1$  if  $s \geq n$ . We attain order  $n + 1$  near the boundary only if

$$\frac{s+1}{2} > n \Rightarrow s > 2n - 1. \tag{3.10}$$

## 4. Numerical results

In order to demonstrate the properties of local solutions we devise a set of numerical experiments. The aim of these is first to show that the computations yield solutions with the claimed asymptotic order, but with better properties than the asymptotic approximation (3.3), and second to demonstrate that the method works also with certain slightly exotic and non-convex shapes. All experiments in this section are performed on the first order formulation (2.4).

We shall investigate three different obstacle geometries: the circle, the ellipse and a *kite*. The kite is a smooth, non-convex obstacle parametrised by  $\kappa(t) = [\sin(2\pi t) + \cos(4\pi t), \cos(2\pi t)]$  for  $t \in [0, 1]$ . The boundary condition is chosen to be either a plane wave or a point-source. From these obstacles and boundary conditions we choose the following test cases:

- (1) A circle of diameter 1, illuminated by an incoming plane wave along the positive  $x$ -axis. See Fig. 3(a). For this case an analytic solution exists which can be used to compute the error [29] and the asymptotic expansion of the form (3.3) can be constructed. Thus we shall be able to assess the asymptotic order of the approximation as well as to investigate break-down of the solutions near shadow boundaries.
- (2) An eccentric ellipse situated at the origin and oriented along the  $x$ -axis, with major and minor axis lengths 1 and  $1/10$  respectively, illuminated by a point-source situated at  $[-1, 1]$ . See Fig. 3(b).
- (3) A kite illuminated by a plane wave traveling along the positive  $x$ -axis, see Fig. 3(c). The illuminated side of the kite is locally convex, whereas the shadow region is non-convex.
- (4) The kite again, this time illuminated by a point-source situated in the point  $[1, 0]$ . See Fig. 3(d). The geometry is non-convex, but such that no multiple reflections occur in a small region near the bottom of the cavity.

In those cases where no analytical solution is available the local solutions are compared to numerical solutions obtained from an efficient full BEM-solver with a fine discretization of around 4000 elements. Details on this solver can be found in [35].

In all examples we efficiently computed the Filon-type quadrature weights (2.20) using a numerical steepest descent method [32] to treat the oscillatory nature of the integrand, combined with generalized Gaussian quadrature [42] to treat its singularities. We refer the interested reader to [30] for results on the rapid convergence of that approach for similar integrals (in particular §7, Example 2).

The local solutions are in all experiments sought in a space of natural splines of order  $s = 5$ . Since the solutions are smooth, only a small number of collocation points ( $\sim 40$ ) are needed to get a good solution. Since spline basis functions are compactly supported, the resulting linear system is banded with bandwidth  $s$ , therefore the linear algebra involved is not a great issue.

We use a wavenumber  $k = 100$  in all experiments unless noted otherwise.

#### 4.1. Comparison of asymptotic methods for the circle

Consider the circular obstacle parametrized by  $\kappa(t) = [\cos(2\pi t), \sin(2\pi t)]$  and illuminated by a plane wave travelling along the  $x$ -axis in the positive direction. The illuminated region corresponds to the range  $t \in [0.25, 0.75]$ . We compute local solutions on an admissible region, say,  $[a, b] = [0.27, 0.73]$ .

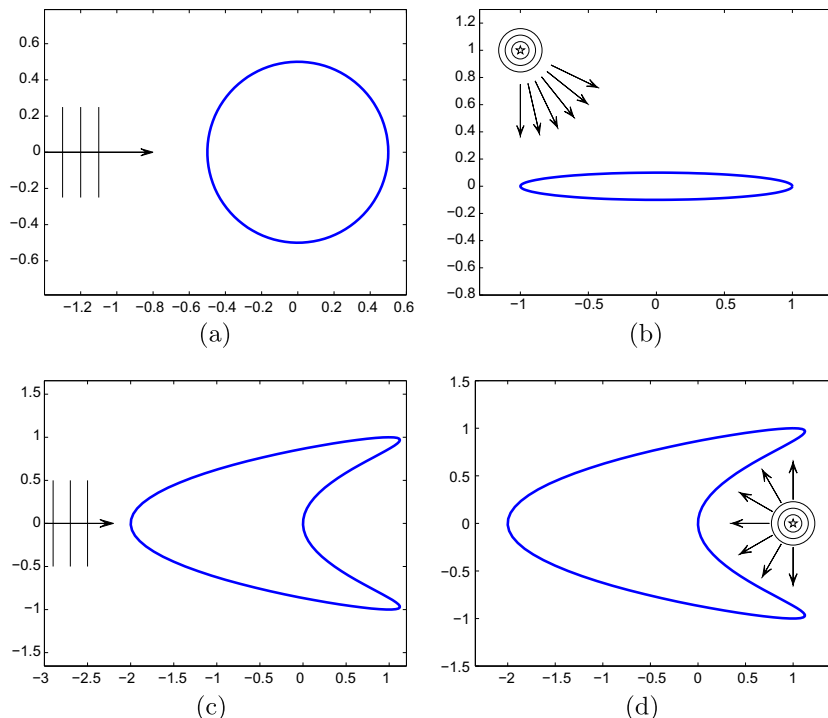


Fig. 3. Four different experimental setups.

Repeating the computation for a range of wavenumbers  $k$ , we can compare the local solution with the asymptotic expansion of the same order in  $k$ . The errors of both asymptotic methods at the point  $t = 0.35$  are compared in Fig. 4 for varying order. The experiments confirm that local solutions have the expected asymptotic order  $\mathcal{O}(k^{-n-1})$ . Moreover, the results show that the local solution is much more accurate than the asymptotic expansion of the solution with the same order when  $n \geq 1$ .

It is well known that the asymptotic expansion (3.3) diverges as one approaches the shadow boundary. Our next experiment shows that this blow-up is not present in the local solution. The relative error for the local solution is shown in Fig. 5 for the whole illuminated region  $t \in [0.25, 0.75]$ , along with the asymptotic expansions of equal order. The results clearly show that the local solutions gracefully loose accuracy near the shadow boundary, whereas the asymptotic expansions blow-up. The accuracy of the local solution even improves with increasing order at the shadow boundaries  $t = 0.25$  and  $t = 0.75$ , though no longer at the rate  $\mathcal{O}(k^{-n-1})$ .

4.2. The case of an eccentric ellipse

For the eccentric ellipse parametrized by  $\kappa(t) = [\cos(2\pi t), \frac{1}{10} \sin(2\pi t)]$  with a point-source at  $[-1, 1]$ , the illuminated region corresponds to the interval  $t \in [0.032, \dots, 0.5]$ . We compute a local solution for the whole illuminated region, excluding some small regions near the shadow boundaries. The result can be seen in Fig. 6. Fig. 6(a) shows the full solution of the scattering problem after phase extraction. The local solution on  $[0.032, \dots, 0.5]$  is superimposed, but the plots are indistinguishable. The relative error of the local solution is shown in Fig. 6(b), by comparing to the solution obtained from the full BEM solver. The accuracy is highest near  $t \approx 0.4$ , but the accuracy improves everywhere with increasing order ( $n = 1, 3$  shown) and with increasing  $k$  (not shown).

4.3. Non-convex scatterers

We present two different cases to show that the method can indeed handle certain cases of non-convex objects. Fig. 7 shows the local solution and the full solution after phase extraction for an incoming plane wave on the kite obstacle, a setup illustrated in Fig. 3(c). We obtain a good approximation on the illuminated part of the kite, which can be viewed as a locally convex part of the scatterer.

The results for a circular wave originating from a point inside the cavity of the kite obstacle are shown in Fig. 8. Due to multiple reflections inside the cavity, the full solution of the scattering problem is not a smooth function after extraction of

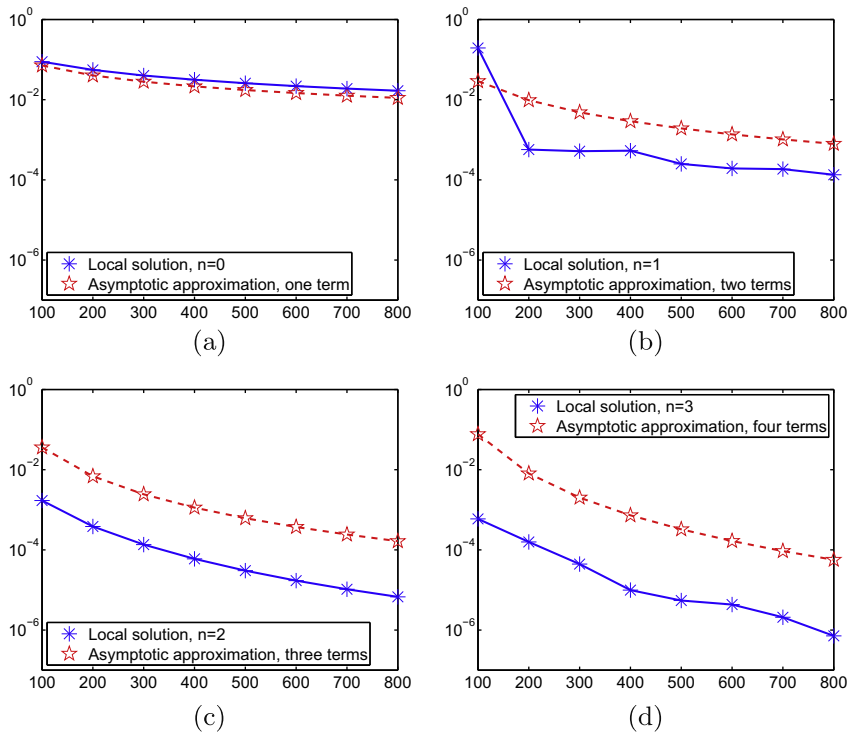
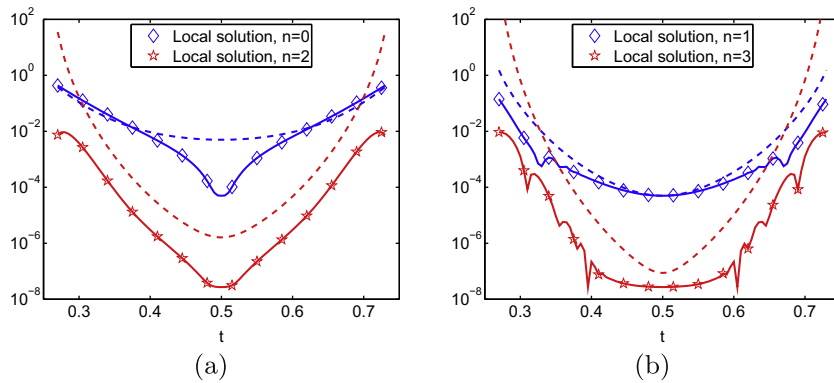
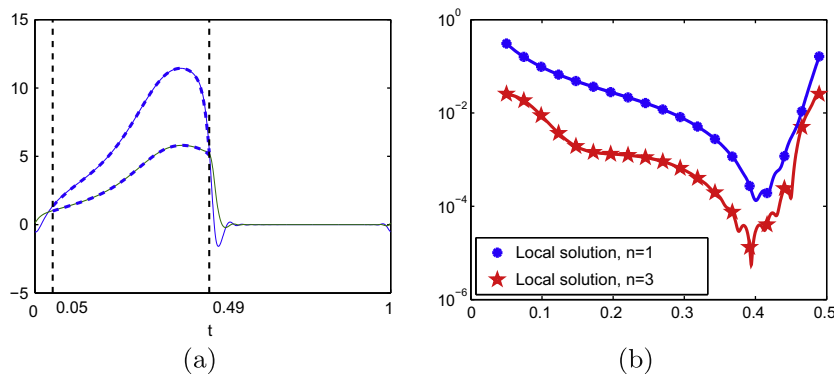


Fig. 4. Relative errors as function of wavenumber for local solutions (solid) and asymptotic expansions (dashed) at  $t = 0.35$  for scattering by a circle. Approximations of order 1, 2, 3 and 4 in panels (a), (b), (c), and (d).



**Fig. 5.** Relative error of local solutions (solid) and asymptotic expansions of equal order (dashed) in the illuminated region of the circle at  $k = 100$ .



**Fig. 6.** Elliptic scatterer with point-source boundary condition,  $k = 100$ : (a) Real and imaginary (divided by 2 in order to separate the curves) parts of the smooth solution with a computed local solution as superimposed dashed curves. (b) For  $n = 1$  and  $n = 3$ , the relative error of the local solution.

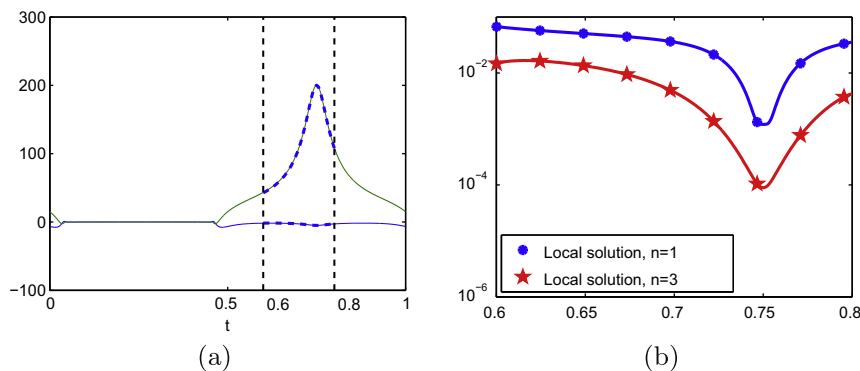


**Fig. 7.** Kite scatterer with a plane wave boundary condition,  $k = 100$ . (a) Real and imaginary parts of the smooth solution  $q_s$ . A computed local solution marked as superimposed dashed curves. (b) For  $n = 1$  and  $n = 3$ , the relative error of the local solution.

the phase of the incoming wave. The “smooth” solution  $q_s$  is in fact highly oscillatory. However, near the bottom of the cavity where no multiple scattering occurs, the phase is well predicted. Fig. 8(a) shows that the local solution actually coincides with the full solution in that region, with small relative error as shown in Fig. 8(b).

Note that both the upper and lower parts of the cavity are admissible and local solutions can be computed for each part. Iterating this procedure, by taking each locally scattered wave on one side of the cavity as the boundary condition for the next local solution on the other side of the cavity, one could conceivably also compute the oscillatory parts of  $q_s$  shown in Fig. 8(a) by adding the fields of a few iterations.

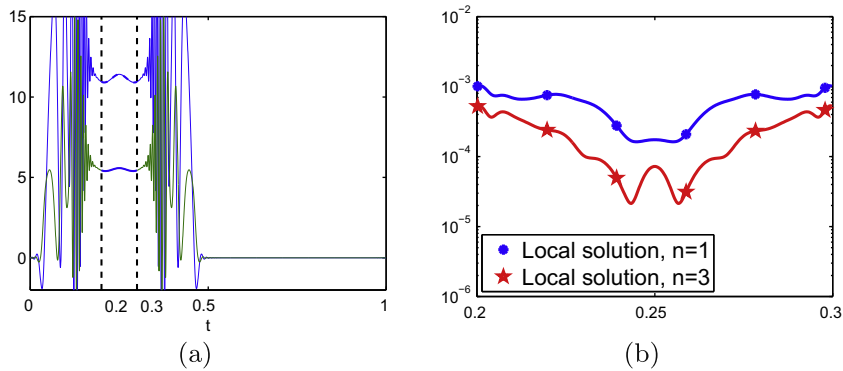


**Fig. 8.** Kite scatterer with a point-source boundary condition,  $k = 100$ . (a) Real and imaginary parts of the smooth solution  $q_s$ . A computed local solution marked as superimposed dashed curves. (b) For  $n = 1$  and  $n = 3$ , the relative error of the local solution.

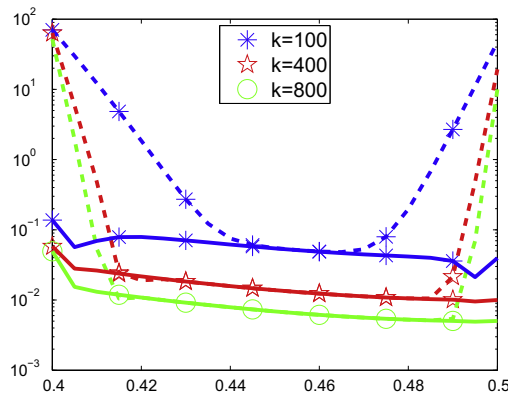


**Fig. 9.** Relative error of a second order finite difference scheme for the local solution for a circular obstacle with an incoming plane wave ( $0.4 < t < 0.5$ ), imposing vanishing second derivatives (solid lines) or homogeneous Dirichlet conditions (dashed lines) at the endpoints.

#### 4.4. Demonstration of boundary layers

Finally, we will show numerically the effect of boundary conditions for Eq. (3.8). We implemented a simple central-difference scheme for the case second order differential equation

$$w_0(t)q(t) + w_1(t)q'(t) + w_2(t)q''(t) = f(t),$$

to compute the local solution for the circular scatterer with an incoming plane wave. Fig. 9 shows the results corresponding to two different sets of boundary conditions: homogeneous Dirichlet (dashed curves) and vanishing second order derivative (solid curves). The accuracy of the computed solution is not severely affected by the boundary condition in the interior of the interval. Near the endpoints however, the boundary layers are visible. The solution corresponding to homogeneous Dirichlet conditions has large errors in an interval near the endpoints that shrinks with increasing  $k$ . The solution with vanishing second order derivatives has bounded derivatives near the endpoints and therefore recovers the slowly varying solution of the singular perturbation problem to high accuracy throughout the interval.

### 5. Concluding remarks

We presented an efficient and simple scheme to compute single reflections in scattering problems to very high accuracy. We reduced the integral equation formulation of a two-dimensional Helmholtz problem to a univariate ordinary differential equation and showed that even simple finite difference schemes can be used to solve this equation. The differential equation appeared due to the use of Filon-type quadrature in the discretization of the integral operator, as Filon-type quadrature employs derivatives of the integrand. The coefficients of the differential equation are given by the weights of the Filon-type quadrature.

Preliminary results were also obtained for three-dimensional scattering problems. A major difference compared to the two-dimensional case is the challenge of efficiently computing the weights of the Filon-type cubature rule. These weights

are given by two-dimensional, singular and highly oscillatory integrals. Current research focuses on their numerical computation based on the results for multivariate oscillatory integrals in [33].

## Acknowledgments

The authors would like to acknowledge insightful discussions on this topic with Valery Smyshlaev (University of Bath), and the many helpful suggestions of the anonymous referees.

## References

- [1] T. Abboud, J.-C. Nédélec, B. Zhou, Méthode des équations intégrales pour les hautes fréquences, *C. R. Acad. Sci. Paris* 318 (1994) 165–170.
- [2] M. Abramowitz, I.A. Stegun, *Handbook of Mathematical Functions with Formulas, Graphs, and Mathematical Tables*, Dover Publications, New York, 1965.
- [3] A. Anand, Y. Boubendir, E. Ecevit, F. Reitich, Analysis of multiple scattering iterations for high-frequency scattering problems. II: the three-dimensional scalar case, Technical Report 147, Max Planck Institute for Mathematics in the Sciences, 2006.
- [4] X. Antoine, M. Darbas, Alternative integral equations for the iterative solution of acoustic scattering problems, *Q. J. Mech. Appl. Math.* 58 (2005) 107–128.
- [5] X. Antoine, M. Darbas, Generalized combined field integral equations for the iterative solution of the three-dimensional helmholtz equation, *ESAIM-M2AN* 41 (1) (2007) 147–167.
- [6] X. Antoine, M. Darbas, Y.Y. Lu, An improved surface radiation condition for high-frequency acoustics scattering problems, *Comput. Methods Appl. Mech. Eng.* 195 (10) (2006) 4060–4074.
- [7] A. Asheim, A combined Filon/asymptotic quadrature method for highly oscillatory problems, *BIT* 48 (3) (2008) 425–448.
- [8] V.M. Babich, V.S. Buldyrev, *Short-Wavelength Diffraction Theory*, Springer-Verlag, Berlin, 1991.
- [9] L. Banjai, W. Hackbusch, Hierarchical matrix techniques for low and high-frequency Helmholtz equation, *IMA J. Numer. Anal.* 28 (1) (2008) 46–79.
- [10] L. Banjai, S. Sauter, A refined Galerkin error and stability analysis for highly indefinite variational problems, *SIAM J. Numer. Anal.* 45 (1) (2007) 37–53.
- [11] A. Bayliss, C.I. Goldstein, E. Turkel, On accuracy conditions for the numerical computation of waves, *J. Comput. Phys.* 59 (1985) 396–404.
- [12] C.M. Bender, S.A. Orszag, *Advanced Mathematical Methods for Scientists and Engineers*, McGraw-Hill, 1978.
- [13] P. Bettess, Short wave scattering, problems and techniques, *Philos. Trans. R. Soc. London A* 362 (2004) 421–443.
- [14] M. Born, E. Wolf, *Principles of Optics*, Cambridge University Press, Cambridge, 1999.
- [15] O.P. Bruno, C.A. Geuzaine, J.A. Monro, F. Reitich, Prescribed error tolerances within fixed computational times for scattering problems of arbitrarily high-frequency: the convex case, *Philos. Trans. R. Soc. London A* 362 (1816) (2004) 629–645.
- [16] O.P. Bruno, L.A. Kunyansky, A fast, high-order algorithm for the solution of surface scattering problems: basic implementation, tests, and applications, *J. Comput. Phys.* 169 (1) (2001) 80–110.
- [17] O.P. Bruno, A. Sei, M. Caponi, High-order high-frequency solutions of rough surface scattering problems, *Radio Sci.* 37 (4) (2002) 2.1–2.13.
- [18] S. Chandler-Wilde, P. Monk, Wave-number-explicit bounds in time-harmonic scattering, *SIAM J. Math. Anal.* 39 (5) (2008) 1428–1455.
- [19] S.N. Chandler-Wilde, I. Graham, Boundary integral methods in high-frequency scattering, in: A. Iserles (Ed.), *Highly Oscillatory Problems: Theory, Computation and Applications*, Cambridge Univ. Press, 2008.
- [20] S.N. Chandler-Wilde, S. Langdon, A Galerkin boundary element method for high-frequency scattering by convex polygons, *SIAM J. Numer. Anal.* 45 (2) (2007) 610–640.
- [21] D. Colton, R. Kress, *Integral Equation Methods in Scattering Theory*, Wiley, New York, 1983.
- [22] P.J. Davis, P. Rabinowitz, *Methods of Numerical Integration*, Computer Science and Applied Mathematics, Academic Press, New York, 1984.
- [23] V. Domínguez, I.G. Graham, V.P. Smyshlyayev, A hybrid numerical-asymptotic boundary integral method for high-frequency acoustic scattering, *Numer. Math.* 106 (3) (2007) 471–510.
- [24] F. Ecevit, F. Reitich, Analysis of multiple scattering iterations for high-frequency scattering problems. I: the two-dimensional case, Technical Report 137, Max Planck Institute for Mathematics in the Sciences, 2006.
- [25] B. Engquist, A. Majda, Absorbing boundary conditions for the numerical simulation of waves, *Math. Comput.* 31 (1977) 629–651.
- [26] B. Engquist, O. Runborg, Computational high-frequency wave propagation, *Acta Numer.* 12 (2003) 181–266.
- [27] M. Ganesh, I. Graham, A high-order algorithm for obstacle scattering in three dimensions, *J. Comput. Phys.* 198 (2004) 211–242.
- [28] C. Geuzaine, O. Bruno, F. Reitich, On the  $O(1)$  solution of multiple scattering problems, *IEEE Transactions Magnetics* 41 (5) (2005) 1488–1491.
- [29] R.F. Harrington, *Time-harmonic Electromagnetic Fields*, McGraw-Hill, New York, 1961.
- [30] D. Huybrechs, R. Coors, On generalized Gaussian quadrature for singular and nearly singular integrals, *SIAM J. Numer. Anal.* 47 (1) (2009) 719–739.
- [31] D. Huybrechs, S. Olver, Highly oscillatory quadrature, in: B. Engquist, A. Fokas, E. Hairer, A. Iserles (Eds.), *Highly Oscillatory Problems: Computation, Theory and Application*, Cambridge Univ. Press, Cambridge, 2009, pp. 25–50.
- [32] D. Huybrechs, S. Vandewalle, On the evaluation of highly oscillatory integrals by analytic continuation, *SIAM J. Numer. Anal.* 44 (3) (2006) 1026–1048.
- [33] D. Huybrechs, S. Vandewalle, The construction of cubature rules for multivariate highly oscillatory integrals, *Math. Comput.* 76 (260) (2007) 1955–1980.
- [34] D. Huybrechs, S. Vandewalle, A sparse discretisation for integral equation formulations of high-frequency scattering problems, *SIAM J. Sci. Comput.* 29 (6) (2007) 2305–2328.
- [35] D. Huybrechs, S. Vandewalle, An efficient implementation of boundary element methods for computationally expensive Green's functions, *Eng. Anal. Boundary Elem.* 32 (8) (2008) 621–632.
- [36] A. Iserles, S.P. Nørsett, Efficient quadrature of highly oscillatory integrals using derivatives, *Proc. R. Soc. London A* 461 (2005) 1383–1399.
- [37] D.S. Jones, An improved surface radiation condition, *IMA J. Appl. Math.* 48 (2) (1992) 163–193.
- [38] J.B. Keller, Geometrical theory of diffraction, *J. Opt. Soc. Am.* 52 (1962) 116–130.
- [39] H.O. Kreiss, Problems with different time scales, *Acta Numer.* (1991) 101–139.
- [40] R. Kress, Minimizing the condition number of boundary integral operators in acoustic and electromagnetic scattering, *Q. J. Mech. Appl. Math.* 38 (1985) 323–341.
- [41] D.P. Levadoux, B.L. Michielsen, New integral formulations for wave diffraction problems, *ESAIM-M2AN* 38 (2004) 157–175.
- [42] J. Ma, V. Rokhlin, S. Wandzura, Generalized Gaussian quadrature rules for systems of arbitrary functions, *SIAM J. Numer. Anal.* 33 (3) (1996) 971–996.
- [43] C.S. Morawetz, D. Ludwig, An inequality for the reduced wave operator and the justification of geometrical optics, *Commun. Pure Appl. Math.* 21 (2) (1968) 187–203.
- [44] J.-C. Nédélec, *Acoustic and Electromagnetic Equations*, Applied Mathematical Sciences, vol. 144, Springer, Berlin, 2001.
- [45] F.W.J. Olver, *Asymptotics and Special Functions*, Academic Press, Inc, New York, 1974.
- [46] V. Rokhlin, Diagonal forms of translation operators for the Helmholtz equation in three dimensions, *Appl. Comput. Harmon. Anal.* 1 (1) (1993) 82–93.
- [47] R. Wong, *Asymptotic approximation of integrals*, SIAM, Philadelphia, 2001.